In situ characterisation of pathogen dynamics during a Pacific Oyster Mortality Syndrome episode

Marion Richard, Jean Luc Rolland, Yannick Gueguen, Julien de Lorgeril, Juliette Pouzadoux, Behzad Mostajir, Beatrice Bec, Sébastien Mas, David Parin, Patrik Le Gall, et al.

To cite this version:

HAL Id: hal-03128530

https://hal.science/hal-03128530

Submitted on 13 Jul 2021

In situ characterisation of pathogen dynamics during a pacific oyster mortality syndrome episode

Marion Richard [a,*], Jean Luc Rolland [b], Yannick Gueguen [b], Julien de Lorgeril [b,e],
Juliette Pouzadoux [b], Behzad Mostajir [c], B´eatrice Bec [c], S´ebastien Mas [d], David Parin [d],
Patrik Le Gall [a], Serge Mortreux [a], Annie Fiandrino [a], Franck Lagarde [a], Gr´egory Messiaen [a], Martine Fortune [a],
Emmanuelle Roque d'Orbcastel [a]

[a] *MARBEC, Univ Montpellier, CNRS, Ifremer, IRD, Sète, France*
[b] *IHPE, Univ Montpellier, CNRS, Ifremer, UPVD, Montpellier, France*
[c] *MARBEC, Univ Montpellier, CNRS, Ifremer, IRD, Montpellier, France*
[d] *OSU-OREME, Univ Montpellier, CNRS, IRD, IRSTEA, Sète, France*
[e] *Ifremer, IRD, Univ Nouvelle-Cal´edonie, Univ La Réunion, ENTROPIE, F-98800 Nouméa,
Nouvelle-Cal´edonie, France*

Abstract

Significant mortality of *Crassostrea gigas* juveniles is observed systematically every year worldwide. Pacific Oyster Mortality Syndrome (POMS) is caused by Ostreid Herpesvirus 1 (OsHV-1) infection leading to immune suppression, followed by bacteraemia caused by a consortium of opportunistic bacteria. Using an *in-situ* approach and pelagic chambers, our aim in this study was to identify pathogen dynamics in oyster flesh and in the water column during the course of a mortality episode in the Mediterranean Thau lagoon (France). OsHV-1 concentrations in oyster flesh increased before the first clinical symptoms of the disease appeared, reached maximum concentrations during the moribund phase and the mortality peak. The structure of the bacterial community associated with oyster flesh changed in favour of bacterial genera previously associated with oyster mortality including *Vibrio, Arcobacter, Psychrobium,* and *Psychrilyobacter*. During the oyster mortality episode, releases of OsHV-1 and opportunistic bacteria were observed, in succession, in the water surrounding the oyster lanterns. These releases may favour the spread of disease within oyster farms and potentially impact other marine species, thereby reducing marine biodiversity in shellfish farming areas

Keywords

1. Introduction

Since 2008, from 40% to 100% *Crassostrea gigas* juveniles in oyster cultures have been decimated annually by Pacific Oyster Mortality Syndrome (POMS) (Garcia et al., 2011; Pernet et al., 2012; Segarra et al., 2010). Pacific Oyster Mortality Syndrome is now reported worldwide (Carrasco et al., 2017; Mineur et al., 2014; Paul-Pont et al., 2014). Together with OsHV-1, *Vibrio splendidus* has also been implicated as a possible pathogen for oyster juveniles (Pernet et al., 2012; Petton et al., 2015b). Using a laboratory-based approach, de Lorgeril et al. (2018) demonstrated that POMS is caused by OsHV-1 infection leading to immune suppression, followed by bacteraemia caused by a consortium of opportunistic bacteria including those belonging to the *Vibrio, Arcobacter, Psychromonas, Psychrobium,* and *Marinomonas* genera. As specified by King et al. (2019), the challenge is now to demonstrate "how the oyster microbiome responds before, during and after an environmental disease outbreak".

Although many studies have explored disease-controlling factors (Petton et al, 2013, 2015a; Whittington et al., 2015a) and the consequences of infection for oysters (Corporeau et al., 2014; Green et al, 2015, 2016; Tamayo et al., 2014), few have investigated the consequences of these mortality events for the environment. Indeed, unlike in most other animal production industries, sick and dead individuals are not separated from conspecifics in shellfish farms, but remain in the rearing environment until their flesh totally disappears (Richard et al. 2017, 2019). The mortality of oyster juveniles has been shown to increase ammonium and phosphate fluxes at the oyster interface (Richard et al., 2017) and to reduce the N/P ratio due to decomposition of the flesh (Richard et al, 2017, 2019). Oyster mortality has been also shown to induce changes in microbial planktonic components during the infection and mortality peak, with proliferation of picophytoplankton and heterotrophic ciliates (*Balanion, Uronema*) (Richard et al., 2019). Ciliates may proliferate in response to a bacterial proliferation associated with decaying oyster tissue (Richard et al., 2019). Beyond disturbing the ecosystem, the fact sick and dead individuals remain in the environment could also favour cross-contamination and disease spread. Indeed, oyster mortality shows strong spatial dependence, starting inside the oyster farm and rapidly spreading beyond (Pernet et al., 2014a). We propose the hypothesis that pathogens released from infected and dead oysters into the water column may be at the origin of disease transmission to naïve oysters, as already shown using a laboratory-based approach with OsHV-1 (Schikorski et al., 2011). To date, no *in-situ* description or quantification is available in the literature on potential pathogen releases during mortality events in ecosystems where shellfish are cultured.

Using an *in-situ* approach in the natural environment, the aim of this study was to demonstrate, (i) temporal OsHV-1 dynamic and microbiota community changes in oyster flesh and (ii) the release of OsHV-1 and opportunistic bacteria from oysters into the water column, before, during and after an oyster mortality episode in the Mediterranean Thau lagoon. These data will advance our understanding of the consequences of the massive and recurrent POMS events for the dynamics of potential pathogens in ecosystems where shellfish are cultured.

2. Material and methods

2.1. Experimental design and devices

As described in the paper by Richard et al. (2019), the experiment was conducted from March to June 2015 in the Thau Lagoon on the French Mediterranean coast (43°22′44.87″N, 3°34′37.64′E). At the end of March 2015, 27,000 juvenile oysters were purchased from SCEA Charente Naissains (Port des Barques, France). The juveniles originated from the Marennes-Ol´eron area (45°58′16.08″N, 01°06′16.2″W), where they were collected on spat collectors in July 2014 and grown until being harvested and shipped to the study site at S`ete for the experiment.

Mean total wet weight (WW) and length (±SD) measured on arrival at the laboratory were 0.49 ± 0.02 WWg and 1.8 ± 0.02 cm, respectively.

After two days of acclimation in laboratory tanks, the juvenile oysters were placed in eighteen lantern nets (∅: 45 cm, H: 105 cm) comprised of seven shelves at a stocking density of 100, 200, 350 individuals per shelf. The 18 lanterns of oyster juveniles were then suspended from an experimental structure (called a table) and immersed one metre below the surface of Thau Lagoon (Fig. 1). The water depth at the site was 4 m.

A first batch of six lanterns was randomly chosen and used to study oyster juvenile mortality and pathogen dynamics in oyster flesh (Figs. 1A and 2A). The lanterns in this batch were randomly distributed in the right-hand part of the table so as to be accessible by boat (Fig. 1A). A second batch of six lanterns of oyster juveniles and two empty lanterns were randomly selected and used to estimate pathogens dynamics and releases into the water column using pelagic chambers (Figs. 1B and 2B). The lanterns were randomly located in the first (5 × 5 m) squares of the table (Fig. 2B). Different batches of lanterns were sampled for Tasks A and B (Figs. 1 and 2) because in Task A, the lanterns had to be removed from the water and placed in the boat for oyster sampling and counting, which probably dispersed decaying flesh and faeces. The lanterns for Task B were left in the water to limit physical disturbance and possible dispersal of decaying oysters and faeces so that the release of pathogens during the decomposition of the flesh could be measured in real conditions. The other six lanterns of oysters were placed near the first batches but were not sampled. These were used to maximise our chances of observing changes in the water column linked to oyster mortality. The abundance of oyster juveniles used in this study (27,000 ind. per 100 m^2, see Fig. 2 for details of the area: 270 ind.m^2) was lower than in shellfish farms where 1200 lanterns containing 350 individuals per storey were suspended per culture table (1200 × 350 x 7: 2,940,000 ind. per 500 m^2: ie. 5880 ind.m^2, see Fig. 2 in Gangnery et al., 2003 for details of the size and structure of a standard culture table in the Thau lagoon).

2.1.1. Task A: oyster juvenile mortality and pathogen dynamics in oyster flesh

Throughout the experiment, on the central shelf, the numbers of living, dead, and moribund oysters in two lanterns per stocking density were counted at weekly intervals (Fig. 1A). As described in Richard et al. (2019), oysters were qualified as (i) dead, when their valves were open at emersion; (ii) alive, when their valves were closed at emersion; or (iii) moribund, when their valves did not close properly and air bubbles escaped when pressure was exerted on the two valves. Dead oysters were removed from the sampled shelf at each sampling point. "Instantaneous" rates of mortality and moribund oysters were calculated each week from the number of dead or moribund individuals on the shelf relative to the total number of oysters observed. Cumulative mortality rates were calculated each week from the sums of dead oysters observed from the beginning of the experiment to the initial number of oysters per shelf. These data were used to identify different steps of the mortality episode termed "before", "starting", "moribund", "mortality" and "post-mortality". In parallel, each week, two batches of three oysters were randomly sampled on the central shelf of each lantern for OsHV-1 and microbiota analysis (7 weeks x 3 densities (100, 200, 250) x 2 lanterns x 2 batches, n = 84) (Fig. 2A).

2.1.2. Task B: Pathogen dynamics in the water column and releases

At weekly intervals before, during, and after the mortality event, four 425-L pelagic chambers (150 cm Height, 60 cm ∅, Fig. 2B) were positioned by divers around two sets of four lanterns either containing no oysters (0: absence), or 100, 200, or 350 oysters (presence: Fig. 2B). During placement, pelagic chambers were first delicately positioned around each lantern (Fig. 1B). Next, the pelagic chambers were closed at the top with a waterproof cap (Figs. 1B and 2B). There was only one lantern per pelagic chamber as shown in Fig. 1 and described in Fig. 2B. The principle behind incubation in the pelagic chambers was to enclose the oysters in a closed system without water renewal. Over time, the oysters would consume the available oxygen via respiration, and the oxygen concentration would consequently decrease. Using this confinement, we were able to measure the exchanges at the interface of the oyster lanterns and determine what is consumed (e.g.,

phytoplankton), excreted (e.g., ammonium, phosphates) or released (e.g., pathogens). To be able to measure these fluxes, the incubation time had to be long enough to induce significant variability of the concentrations observed at the beginning and end of incubation without stressing the oysters. In this study, incubation was limited to 5 h to enable measurement of significant pathogen releases without causing physiological stress to the juvenile oysters. Oxygen depletion did not exceed 20% and oxygen levels always remained above 70% according to the values recorded by each of the HOBO U26 Dissolved Oxygen loggers (Fig. 1B). Water was sampled from each pelagic chamber at the beginning and end of the five-hour-incubation period (T0, Tf; Figs. 1B and 2B) at each stocking density and in each sampling week for the analysis of OsHV-1 and microbiota analysis in the water column. The water was sampled in the pelagic chamber using a tube, a peristaltic pump and a series of plastic bottles (previously cleaned with 1N chlorhydric acid), from a platform as shown in Fig. 1C. At the end of the incubation, the pelagic chambers were removed and placed in the boat, then, back at the laboratory, were cleaned, and stored until the following sampling session. Each sampling week in 2015 was attributed a number (W16 to W22). W16 corresponded to the 13–19th of April, W17 to the 20–26th of April, W18 to 27th of April-3rd of May, W19 to 4–10th of May, W20 to 11–17th of May, W21 to 18–24th of May, and W22 to 25–31st of May, 2015.

2.2. Sampling

2.2.1. Oysters
Oyster juveniles were transported to the lab in coolers. They were measured with a calliper and weighed to 10^{-3} g on a precision balance. They were dissected. Two batches, comprising the flesh of three oysters were randomly combined in two Eppendorf tubes to produce two samples per lantern for DNA extraction. The Eppendorf tubes were filled with 100% ethanol and stored at − 20 °C.

2.2.2. Water
The water samples were transported to the lab in plastic bottles in coolers. Water samples (500 ml) taken at T0 and Tf, were vacuum filtered using 0.22 µm (Acetate Plus) membranes to dissociate free forms of OsHV-1 from those associated with living and non-living particles. The membranes were placed in Eppendorf tubes filled with 100% ethanol and kept at − 20 °C. The 0.22 µm-filtered water samples were placed in 50-ml sterile tubes and kept at − 20 °C. The samples taken at T0 in the absence of oysters (0) were used to describe the dynamics of OsHV-1 and microbiota in the water column over time (6 weeks x 2 lanterns, n = 12). The samples taken at Tf were used to compare and quantify changes in OsHV-1 levels and microbiota composition in the water in the pelagic chamber in the presence and in the absence of oysters over time (5 weeks (no Tf data in W16) x 4 densities (0, 100, 200, 350) x 2 lanterns, n = 40).

Quantification of OsHV-1 and microbiota analyses were conducted from common DNA extractions of the same samples of oyster flesh and water.

2.3. Nucleic acid extraction
Environmental DNA from the filters was extracted and purified using the standard current molecular biology protocols described in unit 2.2.1 (Ausubel et al., 2003). Total DNA from oyster tissues was extracted and purified using the Wizard® SV Genomic DNA Purification System (Promega). Briefly, using a pellet mixer, oyster flesh samples were homogenised on ice in a 1.5-mL microtube containing a digestion solution (10 mM Tris-Base, pH 8, 100 mM NaCl, 25 mM EDTA dihydrate, 0.5% SDS, 0.1 mg/mL proteinase K), and then incubated at 55 °C overnight. The remaining oyster tissues were centrifuged at 2000 g for 2 min and DNA was extracted from the supernatant according to the manufacturer's instructions. After purification, the DNA from the oyster tissues and filters was kept in 100 µL of DNAse/RNAse-Free distilled water at − 20 °C until qPCR and 16S rDNA barcoding.

The concentration and purity of the DNA were checked with a Nanodrop ND-1000 spectrometer (Thermo Scientific).

2.4. Quantification of OsHV-1

Ostreid herpesvirus type 1 genomic DNA was detected and quantified using quantitative PCR (qPCR). A LightCycler® 480 System (Roche) was used for qPCR with the following programme: enzyme activation at 95 °C for 10 min, followed by 40 denaturation cycles (95 °C, 10 s), hybridisation (60 °C, 20 s) and finally elongation (72 °C, 25 s). The PCR reaction volume used was 6 μL. Each volume contained LightCycler 480 SYBR Green I Master mix (Roche), 100 nM of pathogen-specific primers and 1 μl of 100 ng sample DNA. Pathogen-specific primer pair sequences were as follows: C9: 5′-GAG GGA AAT TTG CGA GAG AA-3′, sense and C10: 5′-ATC ACC GGC AGA CGT AGG-3′, antisense (Pepin et al., 2008′). Subsequently, an amplicon melting temperature curve was generated to check the specificity of the amplification products. The absolute number of viral DNA copies of OsHV-1 was estimated by comparing the observed Cq values to a standard curve of the C9-C10 amplification product cloned into the pCR2.1-TOPO vector (Green and Montagnani, 2013). Viral DNA copy numbers were reported with respect to sampled flesh weight and filtered water volume expressed per g^{-1} or mL^{-1}.

Variations in OsHV-1 DNA copies over time were calculated based on the absence (Equation (1)) and presence of oyster juveniles (Equation (2)) according to the following equations where V corresponds to the volume of the chamber (425 L):

(1) Absence: $(CopiesC9C10.lantern^{-1}. h^{-1})$ = ([0: absence]Tf –[0: absence]T0)/(Tf-T0) x V
(2) Presence: $(CopiesC9C10.lantern^{-1}. h^{-1})$ = ([presence]Tf – [absence]T0)/(Tf-T0) x V

2.5. Analysis of bacterial microbiota

For each sample, 16S rDNA amplicon libraries were generated using the 341F-CCTACGGGNGGCWGCAG and 805R-GACTACHVGGGTATCTAATCC primers targeting the variable V3–V4 loops for bacterial communities (Klindworth et al., 2013). Before the library was constructed, DNA was purified a second time using the Macherey-Nagel tissue kit (reference 740952.250) according to the manufacturer's instructions. Paired-end sequencing with a 250-bp read length was performed at the "Bio-Environnement" UPVD technology platform (University of Perpignan Via Domitia Perpignan, France) on a MiSeq system (Illumina) using v2 chemistry according to the manufacturer's protocol. The FROGS pipeline (Find Rapidly OTU with Galaxy Solution) implemented on a galaxy instance was used for data processing (Escudi´e et al., 2018). In brief, paired reads were merged using FLASH (Magoˇc and Salzberg, 2011). After denoising and primer/adapter removal with Cutadapt (Martin, 2011), clustering was performed with SWARM, which uses a clustering algorithm with a threshold (distance = 3) corresponding to the maximum number of differences between two OTUs (Mah´e et al., 2014). Chimeras were removed using VSEARCH (Rognes et al., 2016). The dataset was filtered for sequences present in minus in 3 samples and the remaining data were rarefied to allow for even coverage across all samples. We then produced affiliations using BLAST against the Silva 16S rDNA database (release 132, Dec 2017) to produce an OTU and affiliation table in the standard BIOM format. Rarefaction curves of the species richness were generated using the R package and the rarefy_even_depth and ggrare functions (McMurdie and Holmes, 2013). We used phyloseq for community composition analysis, to infer alpha diversity metrics at the OTU level, as well as beta diversity (between sample distance) from the OTU table. Community similarity was assessed by principal coordinate analysis (PCoA) using the Bray-Curtis dissimilarity.

2.6. Statistical analyses

PERMANOVA was used to test the influence of the sampling week and of the density and their interaction (Week x Density) on mortality rates and OsHV-1 concentrations in oyster flesh and in the water column. Given that oyster density (100, 200, 350) was not found to affect mortality rates and OsHV-1 concentrations in oyster

flesh and the water column, the effect of week, oyster presence (0: absence vs. presence: 100, 200, 350) and their interactions (Week x Presence) on OsHV-1 fluxes were tested to demonstrate the effect of oysters on OsHV-1 and bacteria releases. *A posteriori* tests were performed to compare individual means with each other when significant variations were observed. Analyses were performed with JMP and PRIMER software, and the PERMANOVA package (Plymouth Routines in Multivariate Ecological Research (Clarke and Warwick, 2001).

Principal coordinate analyses (PCoA, {phyloseq}) were computed to represent dissimilarities between samples using the Bray-Curtis distance matrix. We used DESeq2 (Love et al., 2014) to identify candidate taxa (OTU rank) with changes in abundances between the initial and different time points of the kinetics (Tf vs. T0 each week for water and W17 to W20 vs. W16 for oyster flesh). Heatmaps of genera with significant changes in abundances were then computed using relative abundances and Multiple Array Viewer software.

3. Results

3.1. Mortality kinetics

As already described by Richard et al. (2019), mortality of juvenile oysters occurred in the Thau lagoon between April and May 2015 (Fig. 3A). Instantaneous rates of mortality and of moribund oysters varied significantly with the week (p = 0.001, n = 42), but not with the density (moribund p = 0.6, mortality p = 0.9, n = 42) or "week x density" interactions (moribund p = 0.9, mortality p = 0.4, n = 42). The number of moribund oysters (32 ± 3%) peaked in week 18 (Fig. 3A) one week before the highest mortality rate was reached in week 19 (32 ± 5%: Fig. 3A). These weeks were thus categorised as "moribund" and "mortality" stages, respectively. At the end of the event (W22), the cumulative mortality rate reached 54.2 ± 1.1%. Based on these results, different periods related to oyster mortality were defined as follows: "before" (W16) "starting" (W17), "moribund" (W18), "mortality peak (W19), "post-peak" (labelled 1, 2, 3 for W20, 21 and 22, respectively; Fig. 3).

3.2. Dynamics of OsHV-1 in oyster flesh and in the water column

Concentrations of OsHV-1 [flesh] (log10 (x+1)) varied significantly according to week and density interactions (p = 0.002) with no significant variation observed among density during W16, W18, W19 and W21, but with higher means for the 100 density in W17 and W20. Significant variations in OsHV-1 [flesh] over time were observed within densities. Mean OsHV-1[flesh] dynamics preceded the mortality dynamics (Fig. 3B). Concentrations of OsHV-1[flesh] (copies.g^{-1}) started to increase from W17 (8.9 × 10^{+04}), during the "starting" period, and reached maximum levels at the "moribund peak" (W18: 1.09 × 10^{+07} copies.g^{-1}), before decreasing from W19 (7.1 × 10^{+06} copies.g^{-1}) to W20 (7.79 × 10^{+04}) and becoming undetectable in W21 (Fig. 3B; Appendix C).

OsHV-1 was quantified in the water column, i.e. associated with living and non-living particles (Suspended Particulate Matter SPM > 0.22 μm), but was not detected in the free form (i.e., in 0.22 μm-filtered water) (Appendix D). The highest mean amount of OsHV-1 [SPM > 0.22 μm] in the absence of oyster (0, T0) was observed in W18 (112.5 ± 86.8 copiesC9C10.mL^{-1}, Fig. 3C), but the temporal dynamics were nevertheless not significant (n = 12, p = 0.062). OsHV-1 amounts [SPM > 0.22 μm] increased during the 5-h incubation period in the presence of oysters in the pelagic chambers. Mean OsHV-1 amounts [SPM > 0.22 μm] in the presence of oysters and at the final time point ranged from 1503 to 23,251 C9C10 copies.ml^{-1} between W17 and W19, with the highest mean observed in W18 (Fig. 3C). Positive fluxes of OsHV-1 DNA copies (C9C10 copies) were observed in the pelagic chambers in presence of oysters, corresponding to the release of OsHV-1 DNA copies from oysters into the surrounding water. Release of OsHV-1 varied significantly according to "oyster presence and week" interactions (p = 0.001, n = 38), with higher means observed in the presence than in the absence of oysters in W18 and W19 (*: Fig. 4). Release of OsHV-1 DNA started in W17, and the highest mean was reached in W18 with 2.1 ± 0.5 × 10^9 copies OsHV-1.oyster lantern^{-1}.h^{-1}. In W19, OsHV-1 release was still significant, but lower, while

no significant OsHV-1 release was observed in W20 and W22 (Fig. 4). Fluxes of OsHV-1 DNA were positively correlated with the concentrations observed in oyster flesh ($R2 = 0.4$; $p < 0.001$, $n = 28$).

3.3. Dynamics of bacterial microbiota in oyster flesh and in the water column

To investigate the dynamics of the oyster flesh and water column microbiota during the disease episode, we analysed total bacterial communities using 16S metabarcoding over the six weeks of the experiment. A total of 7,011,267 reads were obtained from 142 libraries (Appendix A, B). After the cleaning steps and filtering, 5,009,278 sequences corresponding to 8391 OTUs were kept for further analyses (Appendix A, B). Notably, the 100 most abundant OTUs accounted for more than 75% of all the sequences. Microbiota OTU richness assessed by a Chao1 index was higher in the sea water samples than in the oyster flesh samples (Anova, d.f. = 1, $p < 2e$-16; Fig. 5A). In addition, the Shannon microbiota alpha diversity index was also significantly higher in water samples (Anova, d.f. = 1, $p < 2e$-15; Fig. 5A), demonstrating that bacterial diversity in sea water was higher than in oyster flesh. Class-level assignment of bacterial OTUs indicated dominance of *Gammaproteobacteria* in oyster flesh samples, whereas the dominant classes in the water samples were *Alphaproteobacteria*, *Actinobacteria* and *Bacteroidia* (Fig. 5B). Lastly, principal coordinate analysis based on the Bray- Curtis dissimilarity index showed partitioning of bacteria (Multivariate Anova, pvalue <1e-04) into communities originating from water or from oyster flesh (Fig. 5C), whereas no partitioning was observed according to density in water (Multivariate Anova, pvalue = 0.12) or in oyster flesh ((Multivariate Anova, pvalue = 0.36). Taken together, these results demonstrate a difference in the bacterial microbiota found in seawater and oyster flesh.

Bacterial communities were analysed and identified at the genera level (Fig. 6) during the POMS episode. The most significant changes in bacterial communities occurred in oyster flesh where several bacterial taxa increased in relative abundance at the onset of mortality (Fig. 6, oyster, clusters I and II). Some genera appeared in W17 during the "starting period" (e.g. *Vibrio* to *Bacteroidia* Fig. 5 Cluster I and *Flavobacterium* to *Sulfurovum,* Fig. 6, oyster, Cluster II) whereas others increased in W18 during the "moribund peak" (*Marinifilacea*, *Psychrilyobacter*, *Arcobacter and Psychrobium* Fig. 6, oyster, cluster I), just before the mortality peak in W19 during which Bacteroides and *Clostridiales* were observed (Fig. 6, oyster, cluster I).

Interestingly, some of the bacteria (cluster I) were also found in the surrounding water during the moribund and/or mortality peaks. Higher relative abundances of the opportunistic bacterial genera (*Vibrio, Roseimarinus, Bacteroidia, Marinifilacea, Psychrilyobacter, Arcobacter, Psychrobium, Bacteroides, Clostridiales* and *Saprospira*) were observed in the water column during the moribund and mortality periods (Fig. 6, Water, Cluster I).

4. Discussion

Pacific Oyster Mortality Syndromes have been reported worldwide and have devastated Pacific oyster (*Crassostrea gigas*) juveniles (Garcia et al., 2011; Mineur et al., 2014; Pernet et al., 2012, 2014a; Segarra et al., 2010). This study is the first to simultaneously describe the dynamics of OsHV-1 loads over time and changes in the microbiota community in oyster flesh *in-situ*, and to document the release of OsHV-1 and opportunistic bacteria from oysters into the water column during a mortality event.

4.1. Temporal dynamics of oyster flesh microbiota

The 54% mortality rate of oyster juveniles recorded in the Thau lagoon from April to May 2015 occurred during the same time period as all the other POMS events that have occurred every year since 2008 (Pernet et al, 2010, 2012, 2014b; Richard et al., 2019), when the water temperature rises to 17 °C (Pernet et al., 2012). The oyster densities observed were not found to have an effect either on the mortality rate, or on herpesvirus dynamics, or on changes in the community of bacteria in oyster flesh. It would be interesting to confirm this result with higher densities (i) at the scale of the lantern, knowing that oyster farmers can introduce up to 600 individuals

per storey, but also (ii) at the scale of the culture tables in the Thau lagoon (see Fig. 2 in Gangnery et al., 2003), where oysters can be reared at a maximum density of 3 million juveniles per 500 m^2 table. OsHV-1 DNA was detected in the flesh of the oysters during the POMS episode. Viral load ranges were comparable to those quantified in oyster flesh during mortality events in France (Pernet et al, 2012, 2014b; Renault et al., 2014), or Australia (Paul-Pont et al, 2013, 2014; Whittington et al., 2015b). OsHV-1 DNA was detected in oyster flesh one week before the first visual symptoms of infection, i.e., dysfunction of valve closure at emersion. The temporal dynamics of the OsHV-1 DNA quantified in oyster flesh could be compared to a Gaussian curve, as already shown for pools of infected oyster juveniles (Richard et al., 2017; D. Schikorski et al., 2011). The phase during which increases were observed may correspond to the replication phase of OsHV-1, thereby compromising the oyster immune system and subsequently leading to bacteraemia and mortality (de Lorgeril et al., 2018b). The descending phase corresponds to periods during which effective control of viral replication is achieved in surviving oysters, as previously observed for oyster juveniles (He et al., 2015). A shift in oyster microbiota in favour of opportunistic bacteria such as *Vibrio, Arcobacter*, *Psychrobium and Psychrilyobacter,* all previously found to be associated with oyster mortality (de Lorgeril et al, 2018a, 2018b; Lasa et al., 2019; Le Roux et al., 2016; Lokmer and Wegner, 2015), was also observed during the POMS episode. As already observed using an experimental infection approach (de Lorgeril et al., 2018b), these results confirmed *in-situ* that disease in juvenile oysters arises from infection involving OsHV-1 and a shift in oyster microbiota in favour of opportunistic bacteria.

4.2. Release of pathogens from oysters into the water column

Although the herpes virus is around 70–80 nm in size (Renault et al., 1994, 2000), protocols used for conditioning and sampling were unable to detect OsHV-1 DNA in the free form in water filtered at < 0.22 μm. By contrast, OsHV-1 DNA combined with suspended matter was detected in the proximity of oyster lanterns in shellfish farms. This suspended matter may correspond to living and non-living particles, but currently, we have no information concerning their size class (pico, nano, microplankton), the composition of the particles (organic, mineral) or their type (procaryotes, eucaryotes). Indeed, we do not know whether OsHV-1 was associated with any type of suspended matter or whether the OsHV-1 was associated with dead oyster tissue and/or organisms involved in their decomposition (bacteria, heterotrophic flagellates, ciliates) whose abundance increased during the mortality episode (Richard et al., 2019). Further studies are thus required to investigate the association of OsHV-1 with particles in the water column to better understand the fate of OsHV-1 and its life cycle in marine environments.

The structure of the bacterial community in oyster flesh differed significantly from that observed in the water column in terms of alpha and beta diversity, with a higher alpha diversity in the water than in the oysters, as previously reported by Lokmer et al. (2016). These differences were associated with the dominance of *Gammaproteobacteria* in oyster flesh vs. *Alphaproteobacteria, Actinobacteria* and *Bacteroidia* in water samples. These results are in agreement with those of Pujalte et al. (1999) and Lokmer et al. (2016), who observed dominance of *Alphaproteobacteria* in water.

This study is original in that it used an *in-situ* approach and pelagic chambers to enable observation of pathogen dynamics in oysters and in the water column during an episode of POMS *in situ*. As observed in laboratory experiments (Evans et al., 2016; Sauvage et al., 2009; D. Schikorski et al., 2011), we confirmed that the OsHV-1 load in the water column increased in proximity to infected oysters. Release of OsHV-1 started one week before the first clinical symptoms were observed and reached maximum values (23,251 $_{C9C10}$ copies.ml^{-1}) when the moribund rate was highest (32 ± 3%). During this "moribund phase", 2 billion viral particles were released per hour and per oyster lantern into the water column. Release of OsHV-1 correlated with the OsHV-1 load observed in oyster flesh, suggesting that moribund and dead infected oysters are major sources of the virus, as suggested by Sauvage et al. (2009). In addition to the release of OsHV-1, we also describe an increase in the

occurrence of several genera of bacteria in the surrounding water during incubation in pelagic chambers in the presence of oysters. These included *Vibrio, Roseimarinus, Psychrobium, Arcobacter, Psychrilyobacter* and *Clostridiales*, all previously shown to be associated with oyster mortality (Clerissi et al., 2020; de Lorgeril et al., 2018b; Lasa et al., 2019; Le Roux et al., 2016; Lokmer and Wegner, 2015). The transfer of these opportunistic bacteria from oysters into the water column reached maximum during the moribund phase and the mortality peak.

An increase in the OsHV-1 load and in opportunistic pathogenic bacteria in the water column may allow spread of the disease in the environment as suggested for OsHV-1 during cohabitation experiments between infected and naïve oysters (Petton et al., 2015a; 2013; Schikorski et al., 2011). Spread of the disease from infected to healthy oysters may be favoured by hydrodynamic currents and connectivity, as previously suggested (Pernet et al, 2012, 2014a) given that strong hydrodynamic connectivity has previously been observed between shellfish farms in the Thau lagoon (Lagarde et al., 2019). Bearing in mind that OsHV-1 and some of the opportunistic bacteria released into the environment are known to cause diseases in other marine species (bivalves, holothurians, fish: Table 1), these transfers of pathogens could cause mortality of larval or juvenile stages of other marine species during POMS. The abundance of these species could thus decrease over time before the latter disappear in the long term. Consequently, we hypothesise that the transfers of pathogens could reduce marine biodiversity in ecosystems exploited by shellfish farming, particularly in confined environments such as the Thau lagoon. The impact of these massive and recurrent POMS events on other species, as well as the role of other ecological compartments on disease spread now needs to be investigated in other types of ecosystems.

5. Conclusion and perspectives

This study demonstrated, for the first time in a natural environment, the successive release of OsHV-1 and opportunistic bacteria from oysters into the water column during a 3-week period, i.e., during a POMS episode. These viral and bacterial transfers into the water column may favour the spread of disease between oysters within farms. Further analyses are required to evaluate the effect of these pathogen releases on other marine organisms to determine the consequences of massive oyster mortality on marine biodiversity in oyster growing ecosystems.

Author contribution

Marion Richard: Conceptualization, Methodology, Sampling, Resources, Formal analysis, Visualization, Supervision, Project Administration, Funding Acquisition, Writing-Original Draft, Writing – Review & Editing, Jean Luc Rolland, Resources, OsHV-1 DNA analysis, Writing – Review & Editing, Yannick Gueguen and Julien Delorgeril, Resources, microbiota analysis, Formal analysis, Visualization, Writing – Review & Editing, Juliette Pouzadoux, microbiota analysis, Formal analysis, Behzad Mostajir, Sebastien Mas, Beatrice Bec, Methodology, Resources ´ and Writing – Review & Editing, David Parin, Methodology, Resources, Patrik Le Gall, Serge Mortreux, Gregory Messiaen and Jocelyne Oheix, ´ Diving sampling, Franck Lagarde, Emmanuelle Roque d'Orbcastel, Diving sampling, Writing – Review & Editing, Martine Fortune, Annie Fiandrino, Sampling.

Declaration of competing interest

The authors declare that they have no known competing financial interests or personal relationships that could have appeared to influence the work reported in this paper.

Appendix A. Supplementary data

Supplementary data to this article can be found online at https://doi.org/10.1016/j.marenvres.2020.105251.

References

Arzul, I., Nicolas, J.L., Davison, A.J., Renault, T., 2001c. French scallops: a new host for ostreid herpesvirus-1. Virology 290, 342–349. https://doi.org/10.1006/ viro.2001.1186.

Arzul, I., Renault, T., Lipart, C., 2001a. Experimental herpes-like viral infections in marine bivalves: demonstration of interspecies transmission. Dis. Aquat. Org. 46, 1–6. https://doi.org/10.3354/dao046001.

Arzul, I., Renault, T., Lipart, C., Davison, A.J., 2001b. Evidence for interspecies transmission of oyster herpesvirus in marine bivalves. J. Gen. Virol 82, 865–870.

Ausubel, F.M., Brent, R., Kingston, R.E., Moore, D.D., Seidman, J.G., Smith, J.A., Struhl, K., 2003. Preparation of genomic DNA from mammalian tissue. In: Sons, J.W. (Ed.), Current Protocol in Molecular Biology. Hoboken, NJ, USA, pp. 2.2.1-2.2.3.

Balebona, M.C., Zorrilla, I., Morinigo, M.A., Borrego, J.J., 1998. Survey of bacterial pathologies affecting farmed gilt-head sea bream (Sparus aurata L.) in southwestern Spain from 1990 to 1996. Aquaculture 19–35.

Carrasco, N., Gairin, I., P´erez, J., Andree, K.B., Roque, A., 2017. A production calendar based on water temperature, spat size, and husbandry practices reduce OsHV-1 μ var impact on cultured pacific oyster *Crassostrea gigas* in the Ebro delta (Catalonia). Mediterranean Coast of Spain 8, 1–10. https://doi.org/10.3389/fphys.2017.00125.

Clarke, K.R., Warwick, R.M., 2001. Changes in Marine Communities: an Approach to Statistical Analysis and Interpretation, second ed. PRIMER-E, Plymouth Marine Laboratory, UK.

Clerissi, C., Lorgeril, J. De, Petton, B., Lucasson, A., Toulza, E., 2020. Microbiota composition and Evenness predict survival rate of oysters confronted to pacific oyster mortality syndrome. Front. Microbiol. 11, 1–11. https://doi.org/10.3389/ fmicb.2020.00311.

Corporeau, C., Tamayo, D., Pernet, F., Qu´er´e, C., Madec, S., 2014. Proteomic signatures of the oyster metabolic response to herpesvirus OsHV-1 μVar infection. J. Proteomics 109, 176–187. https://doi.org/10.1016/j.jprot.2014.06.030.

de Lorgeril, J., Escoubas, J.M., Loubiere, V., Pernet, F., Le Gall, P., Vergnes, A., Aujoulat, F., Jeannot, J.L., Jumas-Bilak, E., Got, P., Gueguen, Y., Destoumieux- Garzon, D., Bachere, E., 2018a. Inefficient immune response is associated with microbial permissiveness in juvenile oysters affected by mass mortalities on field. Fish Shellfish Immunol. 77, 156–163. https://doi.org/10.1016/j.fsi.2018.03.027.

de Lorgeril, J., Lucasson, A., Petton, B., Toulza, E., Montagnani, C., Clerissi, C., Vidal- Dupiol, J., Chaparro, C., Galinier, R., Escoubas, J.M., Haffner, P., Degremont, L., Charriere, G.M., Lafont, M., Delort, A., Vergnes, A., Chiarello, M., Faury, N., Rubio, T., Leroy, M.A., Perignon, A., Regler, D., Morga, B., Alunno-Bruscia, M., Boudry, P., Le Roux, F., Destoumieux-Garzn, D., Gueguen, Y., Mitta, G., 2018b. Immune-suppression by OsHV-1 viral infection causes fatal bacteraemia in Pacific oysters. Nat. Commun. 9 https://doi.org/10.1038/s41467-018-06659-3.

Deng, H., He, C., Zhou, Z., Liu, C., Tan, K., Wang, N., Jiang, B., Gao, X., Liu, W., 2009. Isolation and pathogenicity of pathogens from skin ulceration disease and viscera ejection syndrome of the sea cucumber *Apostichopus japonicus*. Aquaculture 287, 18–27. https://doi.org/10.1016/j.aquaculture.2008.10.015.

Escudie, F., Auer, L., Bernard, M., Mariadassou, M., Cauquil, L., Vidal, K., Maman, S., Hernandez-Raquet, G., Combes, S., Pascal, G., 2018. FROGS: Find, rapidly, OTUs with galaxy solution. Bioinformatics 34, 1287–1294. https://doi.org/10.1093/ bioinformatics/btx791.

Evans, O., Hick, P., Whittington, R.J., 2016. Distribution of Ostreid herpesvirus-1 (OsHV- 1) microvariant in seawater in a recirculating aquaculture system. Aquaculture 458, 21–28. https://doi.org/10.1016/j.aquaculture.2016.02.027.

Gangnery, A., Chabirand, J.-M., Lagarde, F., Le Gall, P., Oheix, J., Bacher, C., Buestel, D., 2003. Growth model of the pacific oyster, *Crassostrea gigas*, cultured in Thau lagoon (Méditerranée, France). Aquaculture 215, 267–290.

Garcia, C., Tébault, A., D´egremont, L., Arzul, I., Miossec, L., Robert, M., Chollet, B., François, C., Joly, J.P., Ferrand, S., Kerdudou, N., Renault, T., 2011. Ostreid herpesvirus 1 detection and relationship with *Crassostrea gigas*

spat mortality in France between 1998 and 2006. Vet. Res. 42, 73. https://doi.org/10.1186/1297- 9716-42- 73.

Gomez-Léon, J., Villamil, L., Lemos, M.L., Novoa, B., Figueras, A., 2005. Isolation of *Vibrio alginolyticus* and *Vibrio splendidus* from aquacultured carpet Shell clam (*Ruditapes decussatus*) larvae associated with mass mortalities. Appl. Environ. Microbiol. 71, 98–104. https://doi.org/10.1128/AEM.71.1.98.

Green, T.J., Montagnani, C., 2013. Poly I: C induces a protective antiviral immune response in the Pacific oyster (*Crassostrea gigas*) against subsequent challenge with Ostreid herpesvirus (OsHV-1 μvar). Fish Shellfish Immunol. 35 (2), 382–388. https://doi.org/10.1016/j.fsi.2013.04.051.

Green, T.J., Rolland, J.-L., Vergnes, A., Raftos, D., Montagnani, C., 2015. OsHV-1 countermeasures to the Pacific oyster's anti-viral response. Fish Shellfish Immunol. 47, 435–443. https://doi.org/10.1016/j.fsi.2015.09.025.

Green, T.J., Vergnes, A., Montagnani, C., de Lorgeril, J., 2016. Distinct immune responses of juvenile and adult oysters (*Crassostrea gigas*) to viral and bacterial infections. Vet. Res. 47, 72. https://doi.org/10.1186/s13567-016-0356-7.

He, Y., Jouaux, A., Ford, S.E., Lelong, C., Sourdaine, P., Mathieu, M., Guo, X., 2015. Transcriptome analysis reveals strong and complex antiviral response in a mollusc. Fish Shellfish Immunol. 46, 131–144. https://doi.org/10.1016/j.fsi.2015.05.023.

King, W.L., Jenkins, C., Seymour, J.R., Labbate, M., 2019. Oyster disease in a changing environment: decrypting the link between pathogen, microbiome and environment. Mar. Environ. Res. 143, 124–140. https://doi.org/10.1016/j. marenvres.2018.11.007.

Klindworth, A., Pruesse, E., Schweer, T., Peplies, J., Quast, C., Horn, M., Glockner, F.O., 2013. Evaluation of general 16S ribosomal RNA gene PCR primers for classical and next-generation sequencing-based diversity studies. Nucleic Acids Res. 41, 1–11. https://doi.org/10.1093/nar/gks808.

Lagarde, F., Fiandrino, A., Ubertini, M., Roque, E., Mortreux, S., Chiantella, C., Bec, B., Bonnet, D., Roques, C., Bernard, I., Richard, M., Guyondet, T., Pouvreau, S., Lett, C., 2019. Duality of trophic supply and hydrodynamic connectivity drives spatial patterns of Pacific oyster recruitment. Mar. Ecol. Prog. Ser. 632, 81–100.

Lasa, A., di Cesare, A., Tassistro, G., Borello, A., Gualdi, S., Furones, D., Carrasco, N., Cheslett, D., Brechon, A., Paillard, C., Bidault, A., Pernet, F., Canesi, L., Edomi, P., Pallavicini, A., Pruzzo, C., Vezzulli, L., 2019. Dynamics of the Pacific oyster pathobiota during mortality episodes in Europe assessed by 16S rRNA gene profiling and a new target enrichment next-generation sequencing strategy. Environ. Microbiol. 21 (12), 4548–4562. https://doi.org/10.1111/1462-2920.14750.

Lavilla-Pitogo, C.R., Baticados, M.C.L., Cruz-Lacierda, E.R., de la Pena, L.D., 1990. Occurrence of luminous bacterial disease of *Penaeus monodon* larvae in the Philippines. Aquaculture 91, 1–13. https://doi.org/10.1016/0044-8486(90)90173- K.

Le Roux, F., Wegner, K., Polz, M., 2016. Oysters and Vibrios as a model for disease dynamics in wild animals. Trends Microbiol. 24, 568–580. https://doi.org/10.1016/ j.tim.2016.03.006.

Li, Y.-F., Xu, J.-K., Chen, Y.-W., Ding, W.-Y., Shao, A.-Q., Liang, X., Zhu, Y.-T., Yang, J.-L., 2019. Characterization of gut microbiome in the Mussel *Mytilus galloprovincialis* in response to thermal stress. Front. Physiol. 10, 1–9. https://doi.org/10.3389/ fphys.2019.01086.

Lokmer, A., Kuenzel, S., Baines, J.F., Wegner, K.M., 2016. The role of tissue-specific microbiota in initial establishment success of Pacific oysters. Environ. Microbiol. 18, 970–987. https://doi.org/10.1111/1462-2920.13163.

Lokmer, A., Wegner, Mathias K., 2015. Hemolymph microbiome of Pacific oysters in response to temperature, temperature stress and infection. ISME J. 9, 670–682. https://doi.org/10.1038/ismej.2014.160.

Love, M.I., Huber, W., Anders, S., 2014. Moderated estimation of fold change and dispersion for RNA-seq data with DESeq2. Genome Biol. 15, 1–21. https://doi.org/ 10.1186/s13059-014-0550-8.

Magoc, T., Salzberg, S.L., 2011. FLASH: fast length adjustment of short reads to improve genome assemblies. Bioinformatics 27, 2957–2963. https://doi.org/10.1093/ bioinformatics/btr507.

Mahé, F., Rognes, T., Quince, C., de Vargas, C., Dunthorn, M., 2014. Swarm: Robust and fast clustering method for amplicon-based studies. PeerJ 2014 1–13. https://doi.org/ 10.7717/peerj.593.

Martin, M., 2011. Cutadapt removes adpter sequences from high-throuhput sequencing reads. Tech. notes 17, 10–12.

McMurdie, P.J., Holmes, S., 2013. Phyloseq: an R package for Reproducible interactive analysis and graphics of microbiome census data. PloS One 8. https://doi.org/ 10.1371/journal.pone.0061217.

Mineur, F., Provan, J., Arnott, G., 2014. Phylogeographical analyses of shellfish viruses: inferring a geographical origin for ostreid herpesviruses OsHV-1 (Malacoherpesviridae). Mar. Biol. 162, 181–192. https://doi.org/10.1007/s00227- 014-2566-8.

Mirella Da Silva, P., Renault, T., Fuentes, J., Villalba, A., 2008. Herpesvirus infection in European flat oysters *Ostrea edulis* obtained from brood stocks of various geographic origins and grown in Galicia (NW Spain). Dis. Aquat. Org. 78, 181–188. https://doi. org/10.3354/dao01874.

Paul-Pont, I., Dhand, N.K., Whittington, R.J., 2013. Influence of husbandry practices on OsHV-1 associated mortality of Pacific oysters *Crassostrea gigas*. Aquaculture 202–214. https://doi.org/10.1016/j.aquaculture.2013.07.038, 412–413.

Paul-Pont, I., Evans, O., Dhand, N.K., Rubio, A., Coad, P., Whittington, R.J., 2014. Descriptive epidemiology of mass mortality due to Ostreid herpesvirus-1 (OsHV-1) in commercially farmed Pacific oysters (*Crassostrea gigas*) in the Hawkesbury River estuary, Australia. Aquaculture 146–159. https://doi.org/10.1016/j. aquaculture.2013.12.009, 422–423.

Pépin, J.F., Riou, A., Renault, T., 2008. Rapid and sensitive detection of ostreid herpesvirus 1 in oyster samples by real-time PCR. J. Virol. Methods 149, 269–276. https://doi.org/10.1016/j.jviromet.2008.01.022.

Pernet, F., Barret, J., Le Gall, P., Corporeau, C., D´egremont, L., Lagarde, F., Pepin, J.F., Keck, N., 2012. Mass mortalities of Pacific oysters *Crassostrea gigas* reflect infectious diseases and vary with farming practices in the Mediterranean Thau lagoon. France. Aquac. Environ. Interact. 2, 215–237. https://doi.org/10.3354/aei00041.

Pernet, F., Barret, J., Marty, C., Moal, J., Le Gall, P., Boudry, P., 2010. Environmental anomalies, energetic reserves and fatty acid modifications in oysters coincide with an exceptional mortality event. Mar. Ecol. Prog. Ser. 401, 129–146. https://doi.org/ 10.3354/meps08407.

Pernet, F., Lagarde, F., Jeanne, N., Daigle, G., Barret, J., Le Gall, P., Quere, C., Roque d'orbcastel, E.R., 2014a. Spatial and temporal dynamics of mass mortalities in oysters is influenced by energetic reserves and food quality. PloS One 9. https://doi. org/10.1371/journal.pone.0088469.

Pernet, F., Lagarde, F., Le Gall, P., Roque d'Orbcastel, E., 2014b. Associations between farming practices and disease mortality of Pacific oyster *Crassostrea gigas* in a Mediterranean lagoon. Aquac. Environ. Interact. 5, 99–106. https://doi.org/ 10.3354/aei00096.

Petton, B., Boudry, P., Alunno-Bruscia, M., Pernet, F., 2015a. Factors influencing disease- induced mortality of Pacific oysters *Crassostrea gigas*. Aquac. Environ. Interact. 6, 205–222. https://doi.org/10.3354/aei00125.

Petton, B., Bruto, M., James, A., Labreuche, Y., Alunno-Bruscia, M., Le Roux, F., 2015b. *Crassostrea gigas* mortality in France: the usual suspect, a herpes virus, may not be the killer in this polymicrobial opportunistic disease. Front. Microbiol. 6, 1–10. https://doi.org/10.3389/fmicb.2015.00686.

Petton, B., Pernet, F., Robert, R., Boudry, P., 2013. Temperature influence on pathogen transmission and subsequent mortalities in juvenile Pacific oysters *Crassostrea gigas*. Aquac. Environ. Interact. 3, 257–273. https://doi.org/10.3354/aei00070.

Pujalte, M.J., Ortigosa, M., Macian, M.C., Garay, E., 1999. Aerobic and facultative anaerobic heterotrophic bacteria associated to Mediterranean oysters and seawater. Int. Microbiol. 2, 259–266. https://doi.org/10.2436/im.v2i4.9224.

Renault, T., Bouquet, A.L., Maurice, J.-T., Lupo, C., Blachier, P., 2014. Ostreid herpesvirus 1 infection among pacific oyster (*Crassostrea gigas*) spat: Relevance of water temperature to virus replication and circulation prior to the onset of mortality. Appl. Environ. Microbiol. 80, 5419–5426. https://doi.org/10.1128/aem.00484-14.

Renault, T., Cochennec, N., Le Deuff, R.M., Chollet, B., 1994. Herpes-like virus infecting Japanese oyster (*Crassostrea gigas*). Bull. Eur. Assoc. Fish Pathol. 14, 64–66.

Renault, T., Le Deuff, R.M., Chollet, B., Cochennec, N., Gerard, A., 2000. Concomitant herpes-like virus infections in hatchery-reared larvae and nursery-cultured spat *Crassostrea gigas* and *Ostrea edulis*. Dis. Aquat. Org. 42, 173–183. https://doi.org/ 10.3354/dao042173.

Richard, M., Bec, B., Vanhuysse, C., Mas, S., Parin, D., Chantalat, C., Le, P., Fiandrino, A., Lagarde, F., Mortreux, S., Ouisse, V., Luc, J., Degut, A., Hatey, E., Fortune, M., Roque, E., Messiaen, G., Munaron, D., Callier, M., Oheix, J., Derolez, V., Mostajir, B., 2019. Changes in planktonic microbial components in interaction with juvenile oysters during a mortality episode in the Thau lagoon (France). Aquaculture 503, 231–241. https://doi.org/10.1016/j.aquaculture.2018.12.082.

Richard, M., Bourreau, J., Montagnani, C., Ouisse, V., Gall, P. Le, Fortune, M., Munaron, D., Messiaen, G., Callier, M.D., Roque, E., 2017. Influence of OsHV-1 oyster mortality episode on dissolved inorganic fluxes : an ex situ experiment at the individual scale. Aquaculture 475, 40–51. https://doi.org/10.1016/j.aquaculture.2017.03.026.

Rognes, T., Flouri, T., Nichols, B., Quince, C., Mah´e, F., 2016. VSEARCH: a versatile open source tool for metagenomics. PeerJ 2016 1–22. https://doi.org/10.7717/ peerj.2584.

Sauvage, C., Pepin, J.F., Lap´egue, S., Boudry, P., Renault, T., 2009. Ostreid herpes virus 1 infection in families of the Pacific oyster, *Crassostrea gigas*, during a summer mortality outbreak: differences in viral DNA detection and quantification using real- time PCR. Virus Res. 142, 181–187. https://doi.org/10.1016/j.virusres.2009.02.013.

Schikorski, D., Faury, N., Pepin, J.F., Saulnier, D., Tourbiez, D., Renault, T., 2011. Experimental ostreid herpesvirus 1 infection of the Pacific oyster *Crassostrea gigas*: kinetics of virus DNA detection by q-PCR in seawater and in oyster samples. Virus Res. 155, 28–34. https://doi.org/10.1016/j.virusres.2010.07.031.

Schikorski, David, Renault, T., Saulnier, D., Faury, N., Moreau, P., Pepin, J.F., 2011. Experimental infection of Pacific oyster *Crassostrea gigas* spat by ostreid herpesvirus 1: demonstration of oyster spat susceptibility. Vet. Res. 42, 27. https://doi.org/ 10.1186/1297-9716-42-27.

Segarra, A., Pépin, J.F., Arzul, I., Morga, B., Faury, N., Renault, T., 2010. Detection and description of a particular Ostreid herpesvirus 1 genotype associated with massive mortality outbreaks of Pacific oysters, *Crassostrea gigas*, in France in 2008. Virus Res. 153, 92–99. https://doi.org/10.1016/j.virusres.2010.07.011.

Tamayo, D., Corporeau, C., Petton, B., Quere, C., Pernet, F., 2014. Physiological changes in Pacific oyster *Crassostrea gigas* exposed to the herpesvirus OsHV-1µVar. Aquaculture 432, 304–310. https://doi.org/10.1016/j.aquaculture.2014.05.023.

Vestrum, R.I., Attramadal, K.J.K., Winge, P., Li, K., Olsen, Y., Bones, A.M., Vadstein, O., Bakke, I., 2018. Rearing water treatment induces microbial selection influencing the microbiota and pathogen associated transcripts of Cod (*Gadus morhua*) Larvae. Front. Microbiol. 9, 1–13. https://doi.org/10.3389/fmicb.2018.00851.

Whittington, R.J., Dhand, N.K., Evans, O., Paul-Pont, I., 2015a. Further observations on the influence of husbandry practices on OsHV-1 µVar mortality in Pacific oysters *Crassostrea gigas*: age, cultivation structures and growing height. Aquaculture 438, 82–97. https://doi.org/10.1016/j.aquaculture.2014.12.040.

Whittington, R.J., Hick, P.M., Evans, O., Rubio, A., Alford, B., Dhand, N., Paul-Pont, I., 2015b. Protection of Pacific oyster (*Crassostrea gigas*) spat from mortality due to ostreid herpesvirus 1 (OsHV-1 µVar) using simple treatments of incoming seawater in land-based upwellers. Aquaculture 437, 10–20. https://doi.org/10.1016/j. aquaculture.2014.11.016.

Figure 1

Schematic drawing of the experimental "table" and location of the different batches of lanterns used for evaluation

A) Mortality rate and pathogen dynamics in oyster flesh (blue batch) and

B) Pathogen dynamics in the water column and releases using the pelagic chamber (green batch). Photographs illustrating A) oyster sampling, B) how the lantern is incubated in the pelagic chamber, and
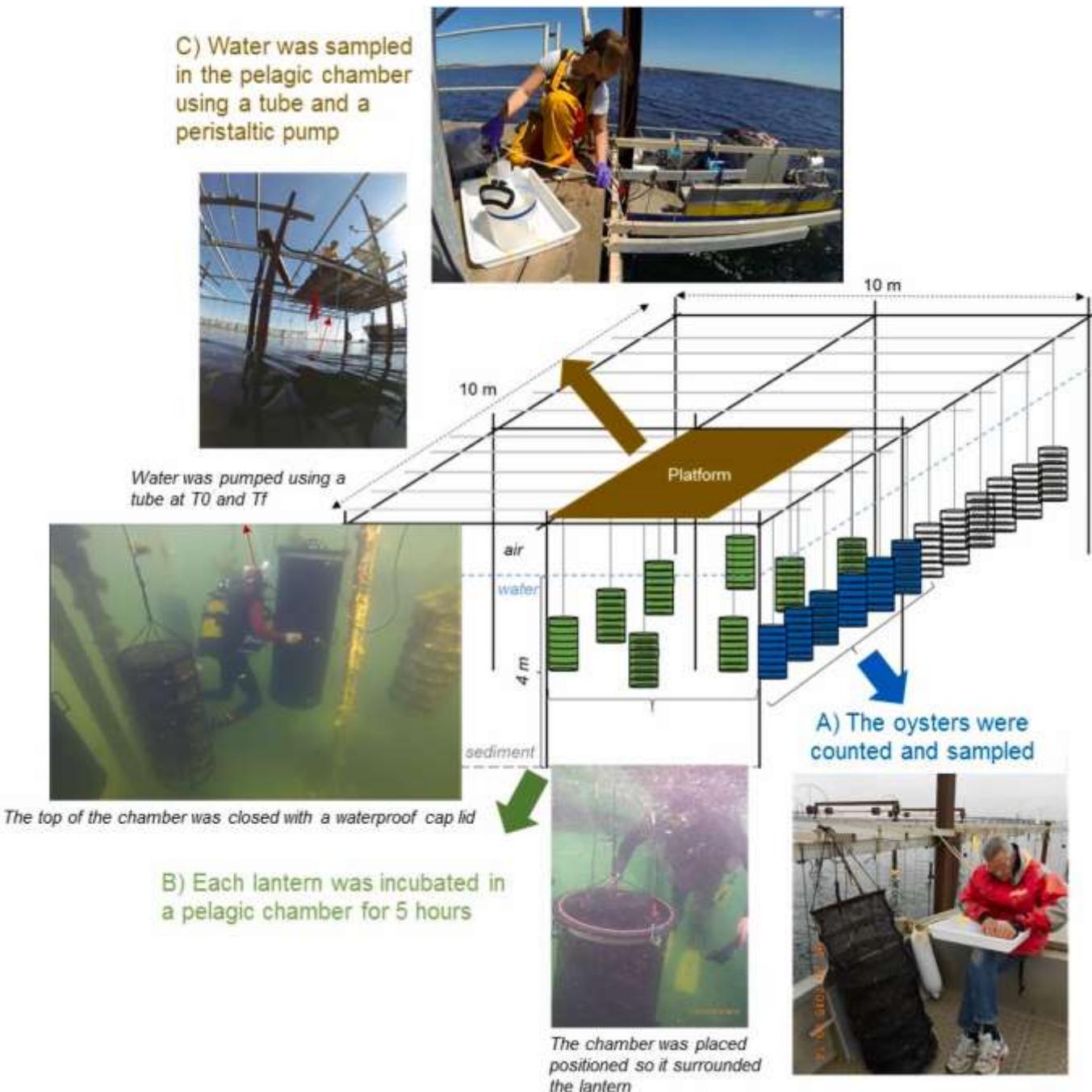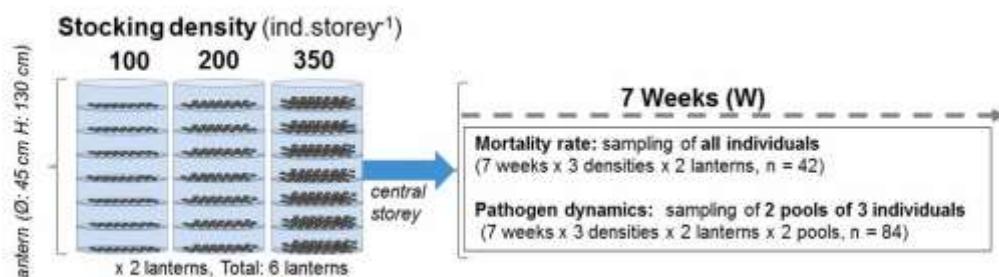
C) water being pumped into the pelagic chamber.

Figure 2

Experimental designs to evaluate

A) Mortality rate and pathogen dynamics in oyster flesh and

B) Pathogen dynamics in the water column and releases. Experimental designs were conducted with 3 or 4 stocking densities (0, 100, 200, 350) to assess absence (0) vs. oyster presence or density (100, 200, 350) over 7 or 6 weeks, depending on the parameter studied (A or B respectively). To estimate pathogen dynamics and releases, the eight lanterns (0, 100, 200, 350) were incubated one a week for 5 h using four pelagic chambers over two days, at a rate of 4 incubations per day. Water was sampled at 2 time points during the incubation: at the initial (T0) and at the final time point (Tf: *i.e.* after 5 h). The diagram and photo illustrate a pelagic chamber composed of a cylindrical tube, a waterproof cap, a water circulation system driven by an independent pump and an oxygen optode probe. Modified from Richard et al. (2019).
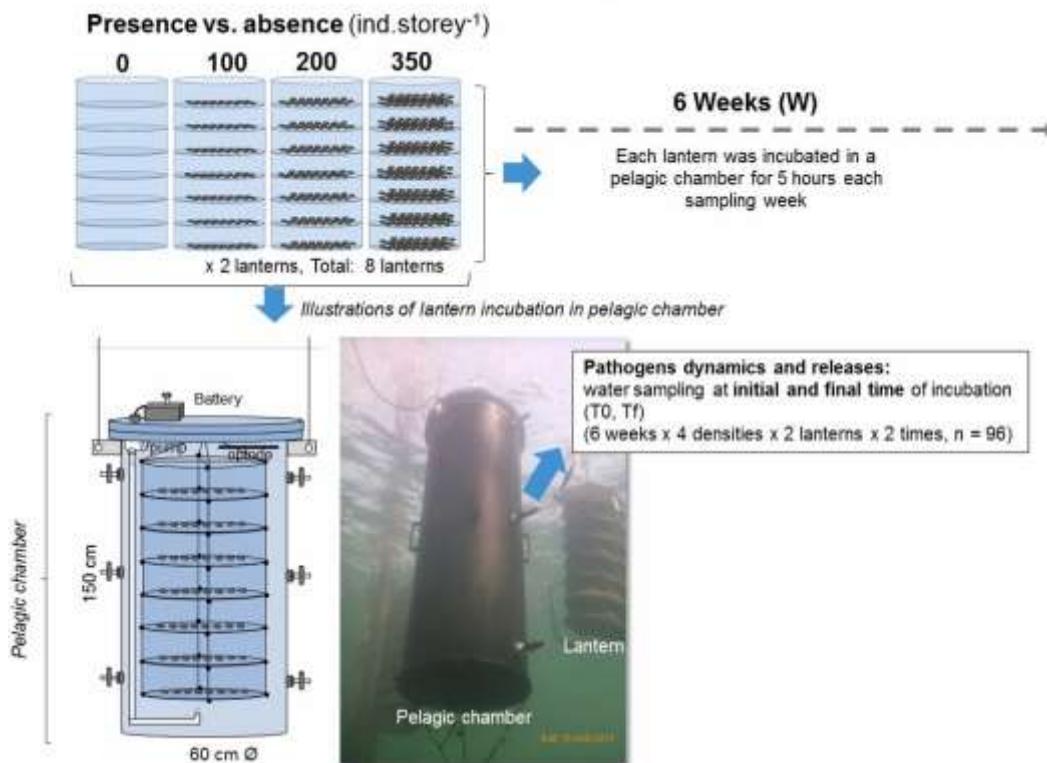
Figure 3

   A) Mean (±SE Standard Error) instantaneous moribund and mortality rates (from Richard et al., 2019),

   B) OsHV-1 concentrations in oyster flesh (Log10 (copies + 1.g⁻¹)) and C) in the water column (i.e. associated with >0.2 µm-Suspended Particulate Matter SPM, copies.mL⁻¹), observed in absence of oysters at the start of incubation (T0: values are on the left axis) and in the presence of oysters at the final incubation time point (Tf: values are on the right axis), according to the sampling week (W16: 13–19th of April, W17: 20–26th of April, W18: 27th of April-3rd of May, W19: 4–10th of May, W20: 11–17th of May, W21: 18–24th of May and W22: 25–31st of May 2015). Different letters indicate significant differences among weeks.
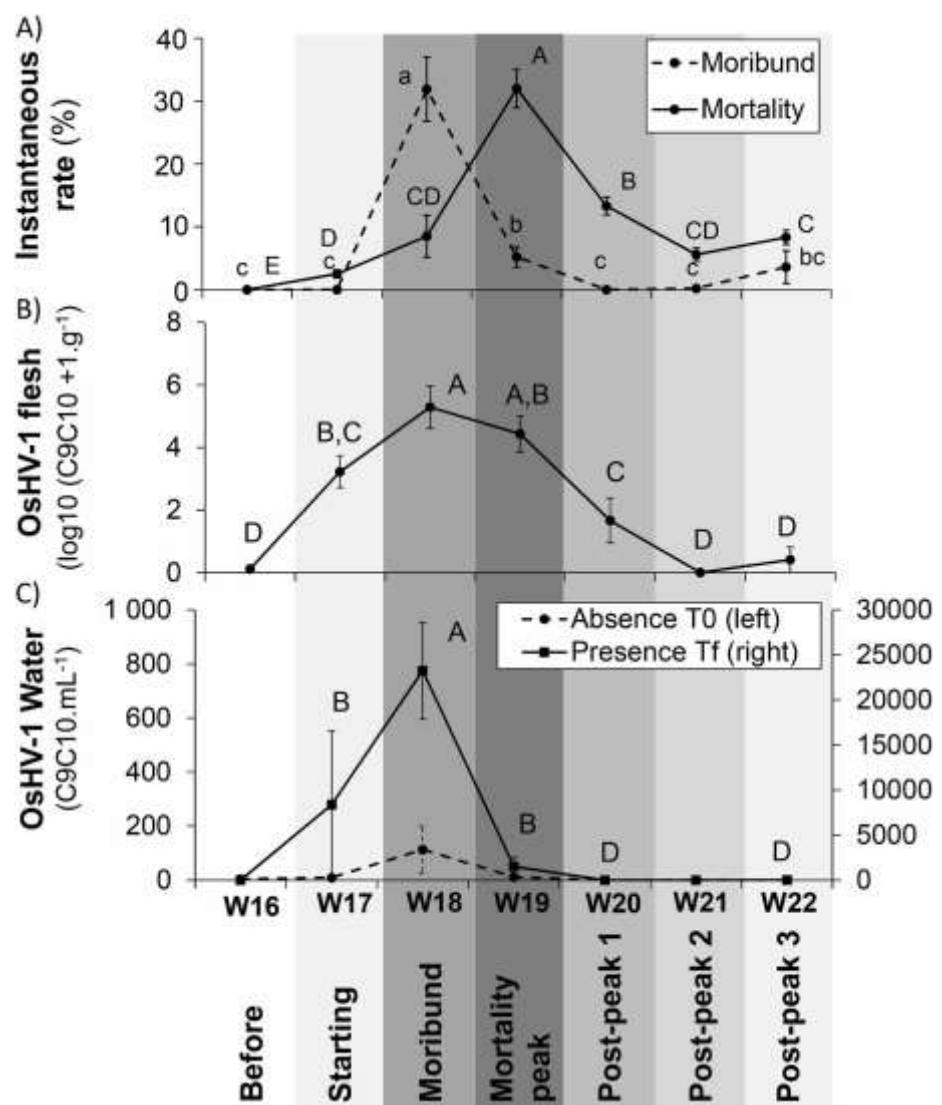
Figure 4

Mean (±SE) OsHV-1 releases from the lanterns into the surrounding water column in presence or absence of oysters according to sampling weeks (W16: 13–19th of April, W17: 20–26th of April, W18: 27 April-3rd of May, W19: 4–10th of May, W20: 11–17th of May, W21: 18–24th of May and W22: 25–31st of May 2015). Different letters indicate significant differences between weeks in the presence of oysters. Stars indicate significant differences according to the absence/presence of oysters in a given week.
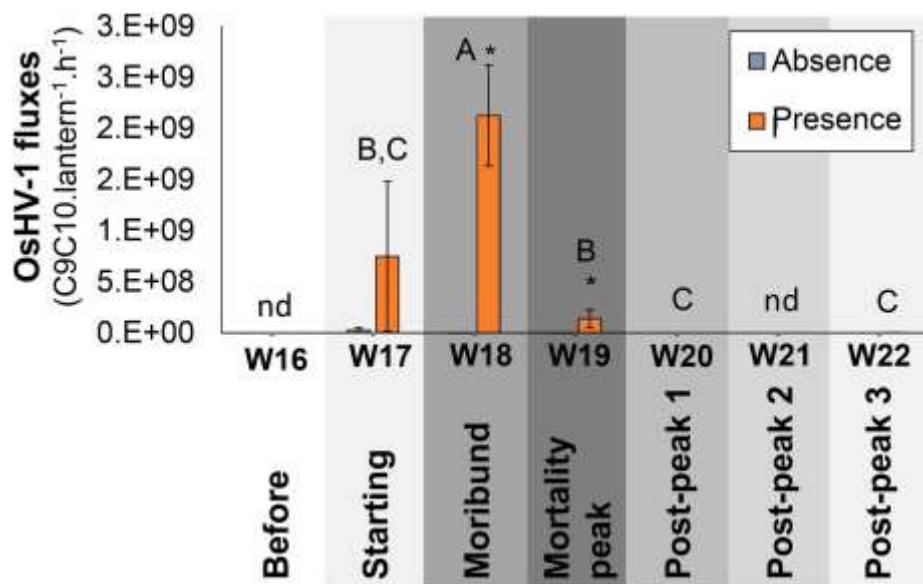
Figure 5

Bacterial microbiota analyses: A) Box plots of alpha diversity (Chao1 and Shannon) indices observed in water and oyster flesh, B) Composition of bacterial communities observed in oyster flesh and in water according to sampling weeks (W16: 13–19th of April, W17: 20–26th of April, W18: 27 April-3rd of May, W19: 4–10th of May, W20: 11–17th of May and W22: 25–31st of May 2015) and C) Principal coordinate analysis (PCoA) plot of the Bray-Curtis dissimilarity matrix comparing oyster flesh and water samples whatever the oyster density (100, 200, 350). The axes of the PCoA represent the two synthetic variables that explained the most variation of the dataset.
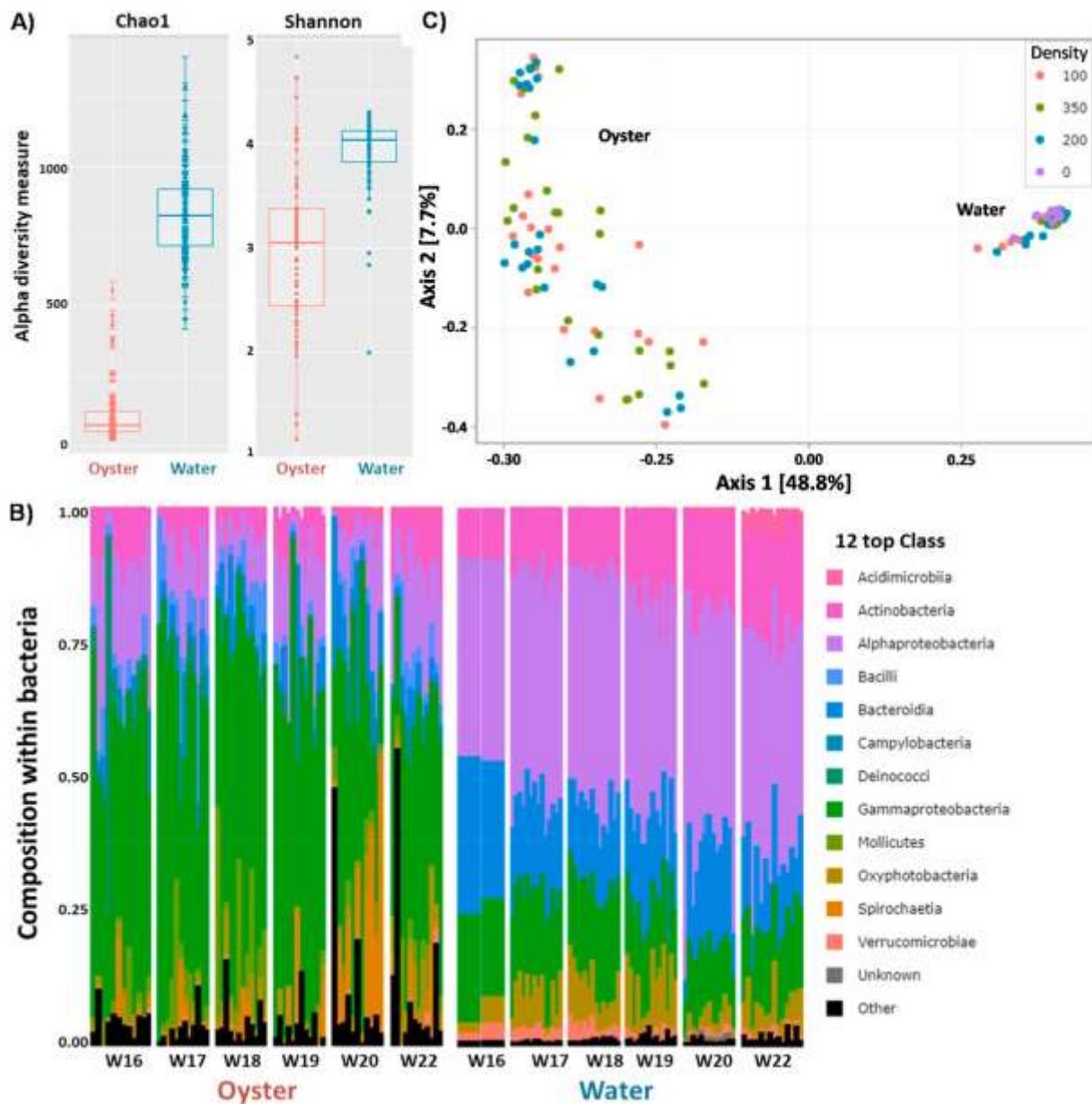
Figure 6

Heatmap of the bacterial genera that significantly changed in relative abundance during the *in-situ* POMS episode. Relative abundances are given for oyster flesh (left part) and for the water column (right part). Sampling weeks are the same as in Fig. 3. Only genera with a relative proportion >5% in at least one sample are shown. The intensity level of the yellow represents the relative abundance of bacterial taxa.
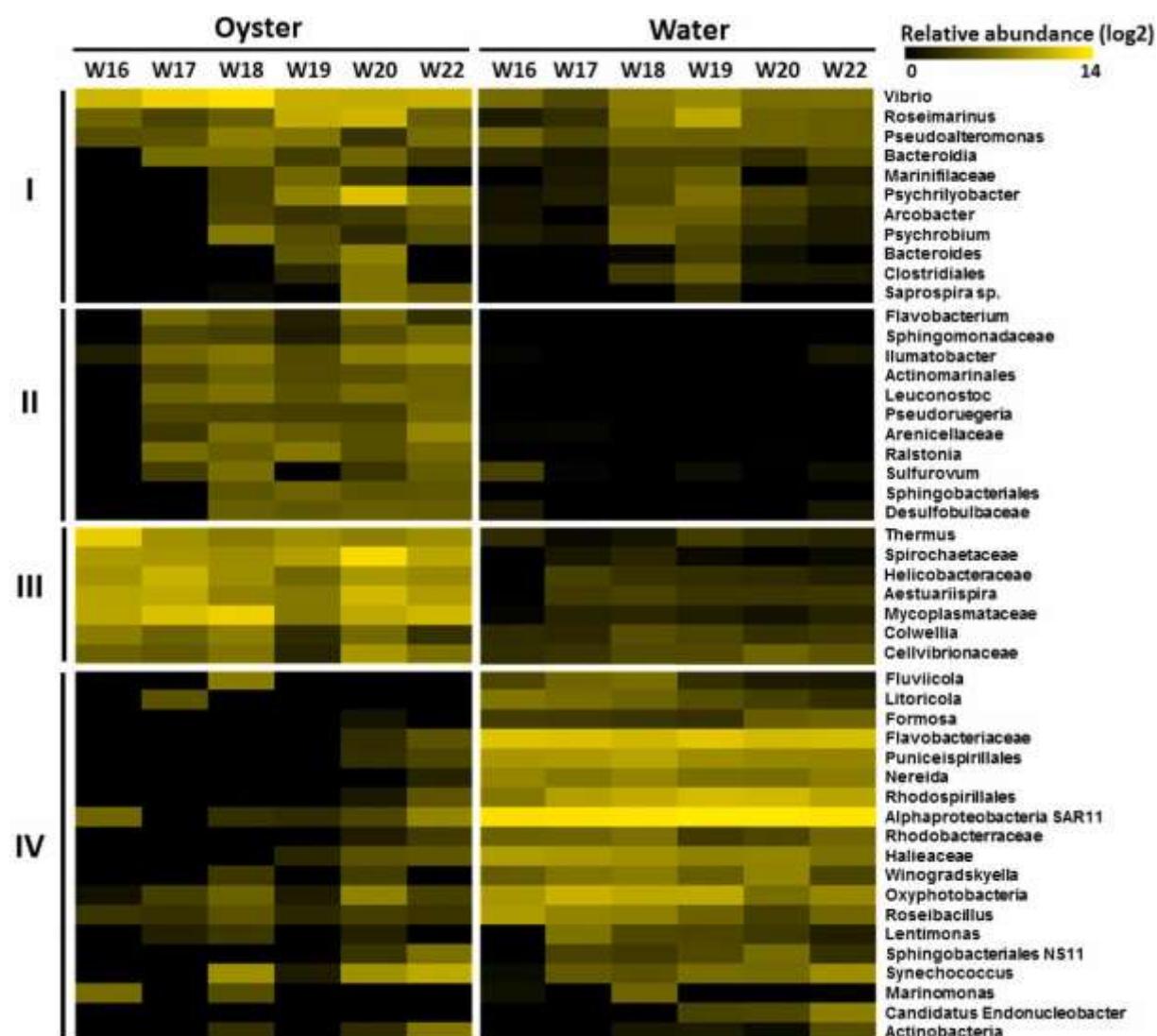
Table 1

A non-exhaustive list of different pathogens found to cause diseases in different marine species (see references) belonging to the list of bacterial genera that were released into the water surrounding the suspended oyster lanterns during the mortality episode studied here.

Pathogen	Species	Host	Species	References
Virus	OsHV-1	European flat	*Ostrea edulis*	Arzul et al. (2001a,b); Mirella Da Silva et al. (2008)
	OsHV-1	Portuguese oyster	*Crassostrea angulata*	Arzul et al. (2001a)
	OsHV-1	Suminoe oyster	*Crassostrea rivularis*	Arzul et al. (2001a)
	OsHV-1	Manila clam	*Ruditapes philippinarum*	Arzul et al. (2001b)
	OsHV-1	carpet shell clam	*Ruditapes decussatus*	Arzul et al. (2001b)
	OsHV-1 μvar	French scallop	*Pecten maximus*	Arzul et al. (2001c)
Vibrio	*Vibrio alginolyticus and Vibrio splendidus*	Carpet shell clam	*Ruditapes decussatus*	Gomez-Leon et al. (2005) ´
	anguillarum,V. alginolyticus,V. harveyi, V. splendidus	Seabream	*Sparus aurata*	Balebona et al. (1998)
	Vibrio harveyi and V. splendidus	Shrimp	*Peneus monodon*	Lavilla-Pitogo et al. (1990)
	Vibrio cyclitrophicus, V. splendidus, V. harveyi, V. tasmaniensis	Holothuria	*Apostichopus japonicus*	Deng et al. (2009)
Arcobacter	*Vibrio & Arcobacter*	Mussel	*Mytilus galloprovincialis*	Li et al. (2019)
	Arcobacter	Cod larvae	*Gadus morhua*	Vestrum et al. (2018)